ISSN: 2716-9227 Algerian Journal of Engineering and Technology 04 (2021) 030–044 e-ISSN: 2716-9278

Algerian Journal of Engineering and Technology

Journal homepage: https://jetjournal.org/index.php/ajet

Original Article

Hexavalent chromium removal from simulated wastewater using biomass-based activated carbon: kinetics, mechanism, thermodynamics and regeneration studies

Umar Yunusa[a,]*, Abdulrahman Ibrahim Kubo[b], Yusuf Abdullahi[c], Tahir Abdullahi[d] and Musa Husaini[a]

[a]Department of Pure and Industrial Chemistry, Bayero University, P.M.B.3011, BUK, Kano-Nigeria
[b]Department of Pure and Applied Chemistry, Adamawa State University, P.M.B. 25, Mubi-Nigeria
[c]Department of Biological Sciences, Yobe State University, P.M.B. 1144, Damaturu. Nigeria
[d]Department of Physics, Yobe State University, P.M.B. 1144, Damaturu. Nigeria

---

ARTICLE INFO

Article history:
Received 03 March 2020
Revised 20 November 2020
Accepted 21 January 2021

Keywords:
Balanites aegyptiaca;
Hexavalent chromium;
Adsorption kinetics;
Mechanism;
Thermodynamics.

ABSTRACT

In this study, activated carbon (ACBA) was fabricated from *Balanites aegyptiaca* seed shell (BASS) using a two-step H_3PO_4 activation approach and was tested for the adsorption of toxic hexavalent chromium [Cr(VI)] from simulated wastewater. The surface properties, morphology, and elemental composition of the prepared ACBA were examined via Fourier transform infrared (FTIR) spectroscopy, scanning electron microscopy (SEM), energy dispersive spectroscopy (EDS), X-ray diffraction (XRD) and Brunauer-Emmett-Teller (BET) surface area analyses. The influence of various operating conditions such as pH, adsorbent amount, contact time and temperature was investigated. Kinetic studies indicated that the pseudo second order model was able to provide a realistic description of the adsorption kinetics and that film diffusion was the dominating mechanism of the sorption process. The adsorption activation energy evaluated using kinetic data suggested physical nature of Cr(VI) adsorption onto the carbon surface. Thermodynamic investigation confirmed that the adsorption was spontaneous and endothermic in nature. Regeneration tests demonstrated that 0.2 M NaOH can appreciably desorb Cr(VI) from Cr(VI)-loaded ACBA and the regenerated adsorbent can be used for six successive adsorption-desorption cycles while sustaining an adsorption efficiency of 80.10%. Altogether, the ACBA showed high adsorptive performance, fast kinetics and reuse potential, indicating the suitability of its application in wastewater treatment.

---

1. Introduction

Because of the increasing global population, water pollution has been an issue of concern for the scientific community for many years. The problem of water pollution is more pronounced in developing nations as the financial resources to provide potable drinking water are grossly inadequate [1]. There has been global awareness for the heavy metal pollution and toxicity in aqueous environment [2]. Many heavy metals such as chromium (Cr), lead (Pb), cadmium (Cd), zinc (Zn) and copper (Cu) are employed in different industrial context and enter the precious aquatic environment whenever they are indiscriminately discarded [3]. The chromium is our main focus here, Chromium is a naturally occurring element found in soil, rocks, animals, plants, and in volcanic gases and dust. Its name is derived

---

* *Corresponding author.*
E-mail address: umaryunusa93@gmail.com

Peer review under responsibility of University of Echahid Hamma Lakhdar.

http://dx.doi.org/10.5281/zenodo.4542410

from the Greek word ‘chroma’ which means color due to the fact that many of its compounds are colored. Chromium can exist in different oxidation states: Cr(0) (metallic chromium), Cr(II) (chromous), Cr(III) (chromic) and Cr(VI) (chromate). Naturally occurring chromium is usually present as trivalent chromium. The relationship between trivalent [Cr(III)] and a hexavalent form [Cr(VI)] of chromium is given by:

$$Cr_2O_7^{2-} + 14H^+ + 6e^- \Leftrightarrow 2Cr^{3+} + 7H_2O + 1.33\ V \qquad (1)$$

The discrepancy in oxidizing potential of these two oxidation states show strong oxidizing power of the Cr(VI) species. On the other hand, high energy needed to oxidize the trivalent form is not available with the biological systems and so almost all the Cr(VI) found in nature are derived from anthropogenic activities [4]. This activities include leather tanning, chromite mining, electroplating, pigment synthesis and metal finishing [5]. Trivalent chromium as an essential trace element in the human diet promotes sugar metabolism but hexavalent is very hazardous for all living things [6,7].

In the aquatic environment, chromium majorly exist in trivalent and hexavalent forms and the relations between them depends strongly on pH and the oxidative properties of the location [8]. In aqueous solution, Cr(VI) exist in the form of; chromate CrO_4^{2-}, dichromate $Cr_2O_7^{2-}$ and hydrogen chromate $HCrO_4^-$. CrO_4^{2-}, is dominant in alkaline medium, $H_2CrO_4^{2-}$ is predominant at pH < 1 while $HCrO_4^-$ and $Cr_2O_7^{2-}$ are predominant at pH 2-6 [9].The following are the important equilibrium reactions for different hexavalent chromium species in aquatic environment [10].

$$H_2CrO_4 \rightarrow H^+ + HCrO_4^- \qquad (2)$$
$$HCrO_4^- \rightarrow H^+ + CrO_4^{2-} \qquad (3)$$
$$2HCrO_4^- \rightarrow Cr_2O_7^{2-} + H_2O \qquad (4)$$
$$HCr_2O_7^- \rightarrow H^+ + Cr_2O_7^{2-} \qquad (5)$$

The International Agency for Research on Cancer (IARC) stated that chromium in the hexavalent form has been deemed to be a class-A human carcinogen [11]. Cr(VI) compounds are 500 times more toxic than the Cr(III) ones due to their high water solubility [12]. In the light of acute toxicity of hexavalent chromium, the US Environmental Protection Agency (EPA) and World Health Organization (WHO) have set maximum allowable limit for Cr(VI) discharge into inland surface water to be 0.1 mg L^{-1} and in potable water to be 0.05 mg L^{-1} [13]. It is highly mobile and is considered acutely toxic, carcinogenic and mutagenic to the living organisms, and hence more hazardous than any other heavy metal [14]. Cr(VI) has been associated with wide range of health problems which include diarrhea, liver damage, skin irritation, asthma, digestive tract and lung cancer, nausea, and vomiting [15,16]. Due to the aforementioned health effects associated to Cr(VI) toxicity, it is mandatory to treat chromium-bearing wastewaters before disposal in to the environment to avoid consequent health problems.

Over the past decades, numerous techniques including precipitation, reverse osmosis, electrodialysis, photocatalysis, chemical oxidation and adsorption have been employed for the treatment of wastewaters [17,18]. Although each technique has its own merits and demerits, adsorption has been quite popular offering flexibility, low cost, easy handling and yielding treated wastewater of appropriate standard for safe disposal [19]. Moreover, the adsorbents can also be recovered by appropriate desorption for reuse [20].

Several studies have focused on various adsorbents for pollutants removal including impregnated alumina, activated carbon, carbon nanotubes, clays, polymeric materials, metal oxides, minerals and resins [21]. Activated carbon is the most popular adsorbent and has been highlighted as one of the best available options in the removal of pollutants from wastewater. Due to its large surface area and controllable pore structure, activated carbon exhibit extremely high adsorption efficiency for many adsorbates. However, its industrial application in wastewater treatment is hampered by its relatively high price and regeneration problems [22].

In the literature, great attention has been given to sourcing cheaper, locally available and renewable materials as precursors for producing activated carbon with comparable functionalities to the commercial product [23,24] . Many agricultural wastes and byproducts including almond shell [25], *Zizuphus jujuba* cores [26], palmyra palm fruit seed [27], rice husk [28], coconut shell [29], palm kernel shell [30], walnut shell [31], apple peels [32], bamboo waste [33] and macadamia nutshell [34] have been employed as precursors for activated carbon production. Continuing the same, here in this work, we have substituted costly commercial activated carbon by activated carbon derived from unconventional, locally available and abundant *Balanites aegyptiaca* seed shell (BASS). BASS has no economic value, and its disposal may cause environmental problems [35,36].

The purpose of this study was to examine the efficacy of activated carbon derived from *Balanites aegyptiaca* seed shell towards the removal of hexavalent chromium from aqueous solution. The physicochemical and textural characterization of the prepared adsorbent was accomplished by using available techniques such as

Fourier transform infrared (FTIR) spectroscopy, scanning electron microscopy (SEM), energy dispersive spectroscopy (EDS), X-ray diffraction (XRD) and Brunauer-Emmett-Teller (BET) surface area analysis. Adsorption kinetics was assessed by fitting the experimental data with the chosen kinetic models. Thermodynamic parameters of activation were estimated using kinetic data at varying temperatures. Furthermore, regeneration studies was carried out to establish the recovery and reuse of the spent adsorbent.

2. Materials and Methods

2.1. Chemicals and Materials

Potassium dichromate ($K_2Cr_2O_7$), sodium hydroxide (NaOH), phosphoric acid (H_3PO_4), nitric acid (HNO_3), sulphuric acid (H_2SO_4), acetic acid (CH_3COOH) and hydrochloric acid (HCl) used were of analytical grade procured from Sigma-Aldrich, Germany. All the chemicals were used as received without further purification. Deionized water was used in the preparation of stock and working solutions. The Cr(VI) stock solution was prepared by dissolving 2.829 g of potassium dichromate in 1 L deionized water in a volumetric flask. The desired experimental concentrations were prepared by appropriate dilution of the stock with deionized water. 0.1 M HCl and 0.1 M NaOH were used to adjust the initial solution pH depending on the requirement. *Balanites aegyptiaca* seed shells for the preparation of activated carbon were sourced from a local market in Gashua-Yobe, Nigeria.

2.2. Methods and Techniques

The activated carbon was synthesized via a two-step chemical activation approach reported by Wang et al. [37]. Briefly, the *Balanites aegyptiaca* shells were dried, ground and screened to obtain a fraction with average particle size of 1 mm. The grounded sample was subsequently carbonized at 700^{o}C in a muffle furnace for 90 min. The carbonized sample was then mixed with 50 % H_3PO_4 solution in a ratio of 3:1 by mass. This was followed by second pyrolysis at 750^{o}C for 90 min. The resulting activated carbon was immersed first in 0.1 M HCl, filtered and then washed thoroughly with hot deionized water until a neutral pH was attained. The adsorbent was dried in an oven at 110°C for 24 h, and then kept in air-tight containers until use. The activated carbon prepared from *Balanites aegyptiaca* seed shells was named as ACBA.

FTIR spectra of ACBA was obtained over a wavenumber range of 4000-600 cm^{-1} using Cary 630 spectrophotometer (Agilent Technologies). The spectra was scanned at a resolution of 8.0 cm^{-1} and with 32 scanning to increase the signal to noise ratio. SEM micrographs were obtained on a Phenomn Pro X scanning electron microscope. Scanning was done at a 1000x magnification and accelerating voltage of 15 kV. The crystallinity of ACBA was observed on a Rigaku Ultima IV powder X-ray diffractometer operated at a current 40 mA and voltage 45 kV with Cu Kα radiation of wavelength 1.5 Å. Scanning was done in the 2Θ range of 10 to 70°. The elemental composition of the sample was elucidated by EDS analysis. The BET surface area, micropore volume and average pore diameter of the adsorbent were estimated by N_2 adsorption method at 77 K, using Quanta Chrome NOVA 2200e, surface area and pore size analyzer. The pH of the aqueous solution was monitored using Jenway 3510 pH meter. Microwave Plasma-Atomic Emission Spectrometer (4210 MP-AES; Agilent) was used for analysis of residual Cr(VI) concentration.

2.3. Batch Adsorption Studies

The influence of the operating parameters namely the solution pH (2–10), adsorbent amount (2–8 g L^{-1}), contact time (5-240 min) and temperature (303–333 K) on the Cr(VI) elimination were investigated in batch mode using Innova 4000 incubator shaker (New Brunswick Scientific) maintained at 150 rpm. In individual experiments, an Erlenmeyer flask was charged with 100 mL of Cr(VI) solution (50 mg L^{-1}) and 0.1 g of the adsorbent was added. The mixture was continuously agitated under room temperature (30 ± 1°C). After a pre-set time interval, the adsorbent was separated from the aqueous phase by centrifugation at 1000 rpm for 5 min using a centrifuge (Centurion series). The residual concentration Cr(VI) in the supernatant was then analyzed by microwave plasma-atomic emission spectrometer. The effect of each parameter was studied through maintenance of constancy of other functions but altering the investigated parameter. For example, thermodynamic parameters for the adsorption were obtained from experiments conducted at various temperatures of 303, 313, 323 and 333 K. The amount of Cr(VI) transferred onto the surface of the adsorbent at equilibrium, qe (mg g^{-1}) and at time t, qt (mg g^{-1}) was calculated using the following relationships.

$$\mathrm{qe} = \left(\frac{\mathrm{Co} - \mathrm{Ce}}{\mathrm{m}}\right)\mathrm{V} \tag{6}$$

$$\mathrm{qt} = \left(\frac{\mathrm{Co} - \mathrm{Ct}}{\mathrm{m}}\right)\mathrm{V} \tag{7}$$

where C_o and C_e are the initial and equilibrium concentration of Cr(VI) in mg L^{-1}, respectively. V (L) is the volume of Cr(VI) solution and m (g) is the dry mass of the adsorbent.

2.4. Regeneration Studies

The regeneration and reusability potential of the spent adsorbent was assessed by agitating 0.1 g of the adsorbent with 100 mL of a Cr(VI) solution (50 mg L^{-1}) for 60 min at 30 °C. After adsorption, the adsorbent was collected, dried and then used for the desorption study. In desorption experiment, the Cr(VI) loaded adsorbent was treated with 100 mL of 0.1 M each of NaOH, HCl, HNO_3, H_2SO_4, CH_3COOH and deionized water (DI) to desorb the adsorbed Cr(VI). The mixture was treated in the same fashion above. The desorption efficiency (%) was computed by the following equation.

$$\text{Desorption efficiency } (\%) = \frac{C_{des}}{C_{ads}} \text{ x } 100 \qquad (8)$$

where C_{des} and C_{ads} represent the amount of Cr(VI) desorbed and adsorbed in mg L^{-1}, respectively. The influence of contact time and desorbing solution concentration on desorption efficiency was investigated using NaOH as desorbing agent. Recycling experiments were conducted according to the above steps. After each cycle, the spent adsorbent was regenerated using 0.2 M NaOH, separated and re-dispersed in Cr(VI) solution. Six consecutive cycles of adsorption-desorption were performed to test the reusability of ACBA.

2.5. Statistical Analysis

To ensure correctness, reliability and reproducibility of the obtained data, all the batch experiments were triplicated and the averaged values of three data set are presented. In nearly all instances, the relative standard deviation was less than 2.0%. In the modeling studies, the coefficient of determination (R^2) and sum of error squares (SSE, %) were employed to evaluate the goodness of fitting and applicability of each model. A higher value of R^2 and lower value of SSE signify better model fitting. The SSE measure the variation between experimental and model predicted values, and it can be computed by the following equation [38]:

$$\text{SSE } (\%) = \sqrt{\frac{\Sigma(q_{e,exp} - q_{e,theo})2}{N}} \qquad (9)$$

where N is the data points number, $q_{e,theo}$ and $q_{e,exp}$ (mg/g) represent the theoretically and experimentally obtained adsorption capacity, respectively.

3. Results and Discussion

3.1. FTIR Spectra XRD Patterns and BET

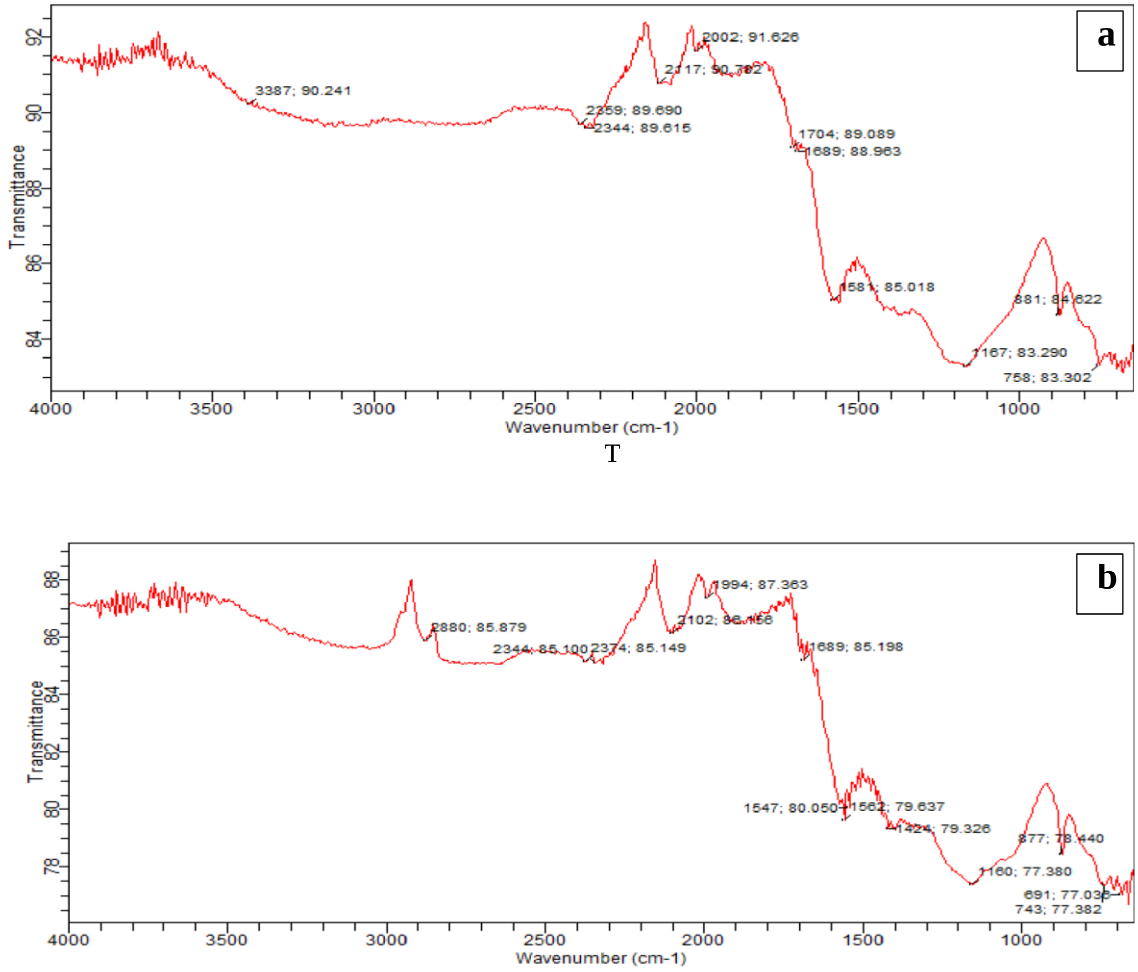

Fig 1. FTIR spectrum of (a) bare ACBA (b) Cr(VI) laden ACBA.

The adsorbent surface functional groups were elucidated by FTIR analysis and the spectrum was displayed in Fig. 1a. The broad band at 3387 cm^{-1} is ascribed to the stretching vibrations of surface OH groups and molecular water [39,40]. The absorption frequency observed at 1704 cm^{-1} was assigned due to the carbonyl group (C=O) of unionized carboxylate stretching of carboxylic acid or ester while the peak at 1689 cm^{-1} was attributed due to the C=O stretching of carboxylic acid with intermolecular hydrogen bonding form [41]. Peaks observed 1562 and 870 cm^{-1} were ascribable to aromatic C-H stretching and free –CSH stretching, respectively [42,43]. The spectrum of ACBA after adsorption exposed changes in the occurrences of some peaks (Fig. 1b). The shift in absorption frequency may be taken as evidence of some sort of interaction between the hexavalent chromium and the adsorbent surface. The XRD pattern of ACBA (Fig. 2) depicts a high degree of amorphosity which may be ascribed to the availability of various volatile organic substances in its structure. The examination of the diffractogram showed the presence of the characteristic peak of graphite positioned at 2ϴ = 25° [44]. The BET surface area, micropore volume and average pore diameter were observed to be 670.35 $m^2 g^{-1}$, 0.268 $cm^3 g^{-1}$, and 29.04 nm, respectively. So, the higher the surface area the better the adsorption performance of ACBA.

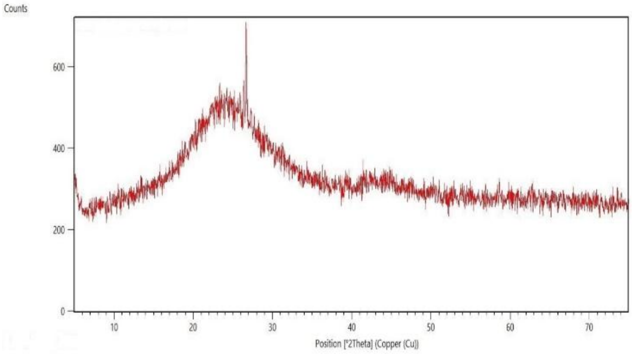

Fig 2. XRD patterns of ACBA

3.2. SEM and EDS Analyses

SEM is an important technique for examining the surface characteristics, especially surface morphology of the adsorbent as it bring out the texture of samples. SEM micrographs of ACBA before and after adsorption are displayed in Figs. 3a and 3b, respectively. Fig. 3a depicts the rough, cracked and pitted surface morphology of the adsorbent which appears to be suitable for adsorption of different adsorbate species. However, a relatively regular and smoother surface was observed after adsorption (Fig. 3b), which signify the occupation of the adsorbent surface by the Cr(VI). The EDS analysis was carried out to ascertain the elemental composition (weight % of elements) of the ACBA (Fig. 4). The obtained results made it possible to demonstrate the presence of carbon at significant percentage (82.13%) compared to other elements such as oxygen (16.27%), nitrogen (1.01%), phosphorus (0.42), silicon (0.10) and chlorine (0.08).

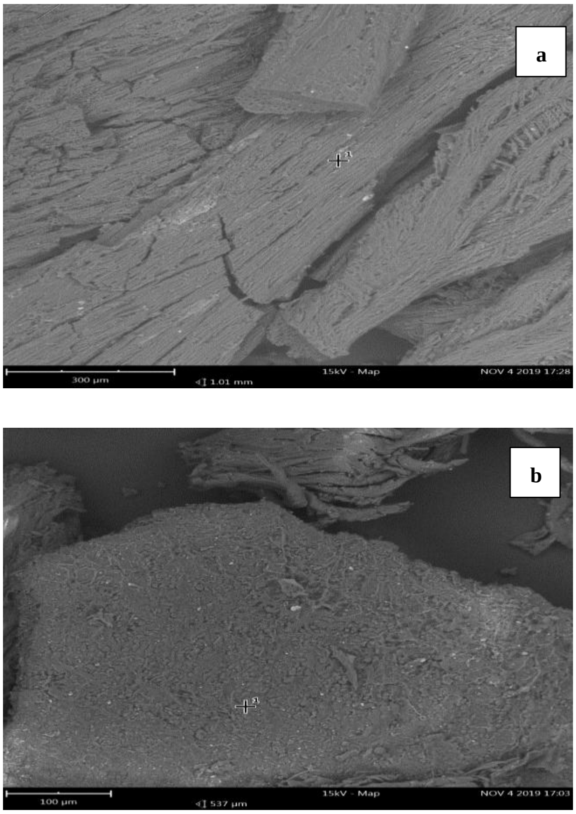

Fig 3. SEM micrograph of (a) bare ACBA (b) Cr(VI) laden ACBA.

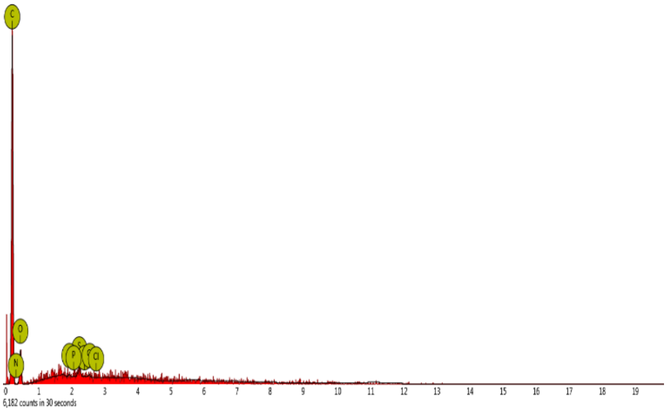

Fig 4. EDS spectrum of ACBA.

3.3. Influence of pH

The pH of the aqueous solution is one of the most sensitive parameters that influence the adsorption of Cr(VI). In the present work, Cr(VI) removal was investigated as a function of pH over a pH range of 2–10 as displayed in Fig. 5. It is obvious from Fig. 5 that the ACBA was more potent in the acidic range and maximum adsorption occurred at pH 2.0. It was observed that there was an appreciable decrease in the adsorption capacity when the pH of the solution was increased from 2.0 to 7.0 and thereafter the impact became negligible. At a lower pH (pH

2.0), the dominant form of Cr(VI) is $HCrO_4^-$ while the surface of the adsorbent is charged positively due to protonation. This result in improved adsorption due to high electrostatic force of attraction. Conversely, the decrease in adsorption of Cr(VI) by increasing the value of pH may be attributed to the dual competition of both the oxyanions of chromium and OH− ions to be adsorbed on the surface of the adsorbent of which OH− predominates [9,14]. In view of the above findings, pH 2.0 was retain as the optimum pH for the rest of the parametric study.

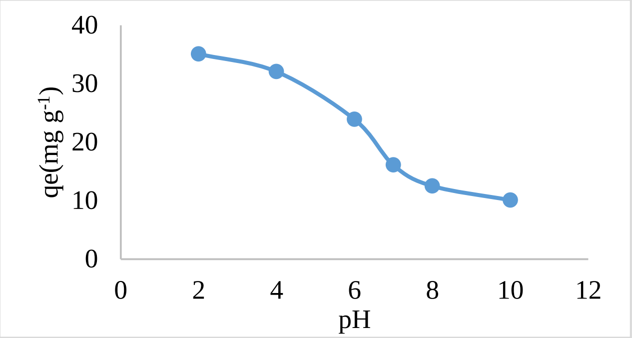

Fig. 5. Influence of pH on Cr(VI) uptake by ACBA (conditions: adsorbent mass = 0.15 g; agitation speed = 150 rpm; time = 60 min; initial concentration = 50 mg L^{-1}).

3.4. Influence of Adsorbent Amount

The influence of ACBA amount on Cr(VI) adsorption, ranging from 0.1 to 0.4 g is displayed in Fig. 6. It is observed that the adsorption capacity decreases from 40.11 to 17.10 mg g^{-1} by increasing the adsorbent amount from 0.1 to 0.4 g.

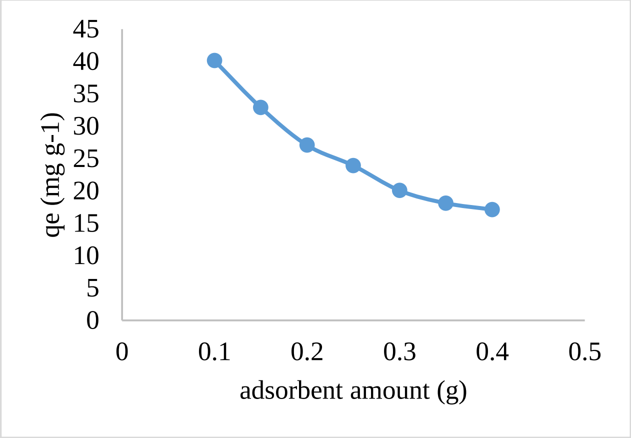

Fig 6. Influence of adsorbent amount on Cr(VI) uptake by ACBA (conditions: pH = 2.0; agitation speed = 150 rpm; time = 60 min; initial concentration = 50 mg L^{-1}).

The decrease in adsorption capacity with increase in amount of adsorbent is basically attributed to the fact that many adsorbent sites remain unoccupied, and ultimately, the adsorption could not reach saturation. Hence, the optimal adsorbent dose of 0.1 g was used for the subsequent experiment.

3.5. Influence of Contact Time and Temperature

Contact time is one of the key parameters for successful deployment of the adsorbent for large scale application [45]. The adsorption data for the uptake of Cr(VI) versus contact time at different temperatures ranging from 303K to 333K is presented in Fig. .7 It can be observed that for all temperatures the adsorption capacity increased with time and, at some point in time, attained a constant value where no more adsorbate was removed from solution. At this point, the amount of hexavalent chromium being adsorbed onto the adsorbent was in a state of dynamic equilibrium with the amount of hexavalent chromium desorbed from the adsorbent. The time needed to achieve this state of equilibrium was termed the equilibrium time (t_e) and the amount of Cr(VI) adsorbed at te depicted the maximum adsorption capacity of ACBA under the employed conditions [46].

The whole adsorption process could be segregated into three regimes (Fig. 7): the adsorption is increased rapidly at early stages (due to substantial adsorption sites and great concentration gradient), and then keeps increasing sluggishly until the equilibrium is attained and remains constant. The second regime is slower because of difficulty in occupying the vacant surface sites due to repulsive forces between the adsorbate in the solid and liquid phases [47]. Sorption of Cr(VI) attained equilibrium in 60 min for the employed range of temperature. The results hinted that the sorption process can be considered fast due to the substantial amount of metal adsorbed onto the adsorbent within the first 30 min of adsorption. It is also evident from Fig. 7 that an increase in temperature results in increased metal uptake and this is valid for an endothermic process. The increase of adsorption capacity with temperature was due to the increase in kinetic energy of adsorbate molecules. Thus, the collision frequency between adsorbate and adsorbent increases, which results in the improved adsorption on the adsorbent surface [48].

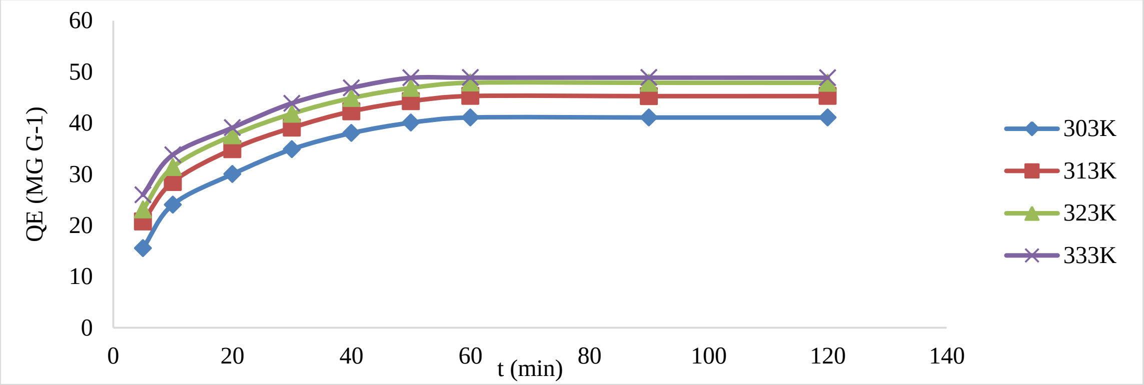

Fig. 7. Cr(VI) uptake against time at various temperatures (conditions: adsorbent mass = 0.1 g; agitation speed = 150 rpm; pH = 2.0; initial concentration = 50 mg L^{-1})

3.6. Adsorption Kinetics

The study of adsorption kinetics is essential for the selection of operating conditions if real water remediation application needs to be explored. It also gives vital information about the solute uptake rate, which is one of the criteria for efficiency of adsorbent [49]. In order to study the dynamic adsorption behavior of the Cr(VI) on ACBA, the pseudo first order and pseudo second order models were employed to simulate the experimental kinetic data.

3.6.1. Pseudo first order kinetic model

This model postulates that the rate of change of adsorbate uptake with time is directly proportional to difference in the amount of adsorbate uptake at equilibrium and at a given time. The pseudo first order rate expression is given by [50]:

$$\frac{dqt}{dt} = k_1(qe - qt) \tag{10}$$

where qe and qt denote the amount of metal adsorbed at equilibrium and at any time t (mg g^{-1}), respectively; k_1 is the rate constant of first order adsorption (min^{-1}).

After integration and applying boundary conditions t = 0 to t = t and qt = 0 to qt = qt, the integrated form of Eq. 10 becomes

$$\mathrm{Log}\left(\frac{qe}{qe-qt}\right) = \frac{k_1}{2.303}t \tag{11}$$

Eq. 11 can be rearranged to obtain the linear form:

$$\log(q_e - q_t) = \log q_e - \frac{k_1}{2.303}t \tag{12}$$

The plot of log (qe-qt) versus t yield a straight line for first order kinetics, which allows computation of rate constant, k_1 from the slope. If the kinetic results do not follow Eq.12, then the experimental data vary in two aspects: (i) k_1 (qe-qt) does not stand for the number of adsorption sites and (ii) log qe is not equal to the intercept of the plot of log (qe-qt) versus t.

Fig. 8 display the fitting plot of pseudo first order model and the computed parameters are exposed in Table 1. The R^2 values of the plots were in the range of 0.9752 to 0.9756. Although the R^2 are satisfactorily high in all cases, the theoretical qe values calculated from this model are comparatively not close to the experimental qe values as evidenced by the high SSE values. This finding is indicative of inapplicability of the pseudo first order kinetic rate expression. The literature data revealed that the first order equation does not match well with the whole range of contact time and is largely applicable over the early stage of the sorption process [51].

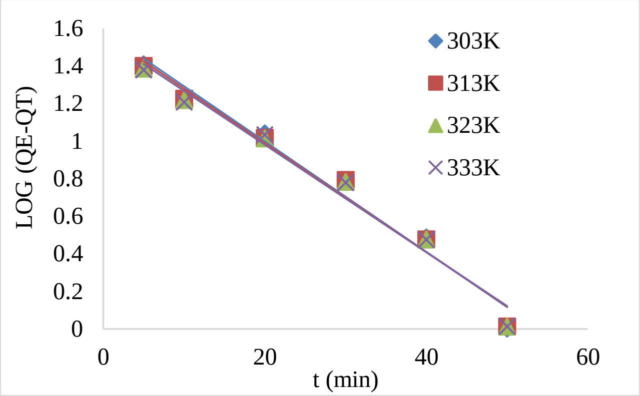

Fig. 8. Pseudo first order fit for Cr(VI) adsorption onto ACBA at varying temperatures

3.6.2. Pseudo second order kinetic model

The pseudo second order model was generally used for the adsorption on solid adsorbents and it rate equation is expressed in differential form as [52]:

$$\frac{dq}{dt} = k_2(qe - qt)^2 \tag{13}$$

where qe and qt denote the amount of metal adsorbed at equilibrium and at any time t (mg g^{-1}), respectively; k_2 represent the rate constant of pseudo first order adsorption (g mg^{-1} min^{-1}).

Integrating Eq. 13 for the boundary conditions t = 0 to t = t and qt = 0 to qt = qt gives

$$\frac{1}{(qe-qt)} = \frac{1}{qe} + k_2t \tag{14}$$

Eq. 14 can be rearranged and linearized to obtain:

$$\frac{t}{qt} = \frac{1}{k_2qe^2} + \frac{t}{qe} \qquad (15)$$

The parameters k_2 and qe can be estimated from the intercept and slope of the plot of t/qt versus t. If the pseudo second order kinetic is applicable, the plot gives a linear relationship. The initial adsorption rate, h (mg g^{-1} min^{-1}), is calculated from the following equation:

$$h = k_2q_e^2 \qquad (16)$$

The plot of t/qt versus t is displayed in Fig. 9, with the relevant parameters determined from the slope and intercept presented in Table 1. It was observed that the rate constant k_2 increased from 2.8 x 10^{-3} to 3.6 x 10^{-3} (g mg^{-1} min^{-1}) with an increase of temperature from 303K to 333K which can be ascribed to the Arrhenius law of temperature dependence of reaction rates. The higher R^2 (>0.9900) and only small difference between $q_{e,theo}$ and $q_{e,exp}$, as reflected by lower SSE (%) values at all temperatures confirmed the kinetic data are well represented by pseudo second order model. The applicability of the pseudo-second-order model suggests that the Cr(VI) is attached on the ACBA surface by chemical bond. From the initial rate of adsorption, h (mg g^{-1} min^{-1}) at varying temperatures, the values of h increased at higher temperatures, signifying the sorption process favors higher temperatures as reflected by higher capacities and rates. The literature report showed that pseudo second order kinetics has been successfully applied to many adsorption systems [53].

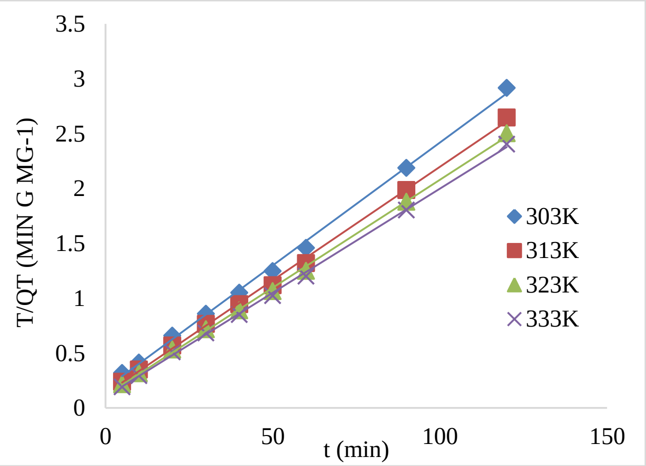

Fig. 9. Pseudo second order fit for Cr(VI) adsorption onto ACBA at varying temperatures

Table 1. Kinetic parameters for Cr(VI) adsorption onto LAC at different temperatures

Kinetic model	parameters	Temperature (K)			
		303	313	323	333
Pseudo-first-order	k_1 (min^{-1})	0.068	0.067	0.066	0.065
	$q_{e\ exp}$ (mg g^{-1})	41.11	45.30	47.90	49.89
	$q_{e\ theo}$ (mg g^{-1})	38.49	37.15	36.05	35.82
	R^2	0.9752	0.9779	0.9778	0.9756
	SSE (%)	1.07	3.33	4.84	5.74
Pseudo-second order	k_2 (g $mg^{-1}min^{-1}$)	2.8 x 10^{-3}	3.3 x10^{-3}	3.4 x 10^{-3}	3.6 x 10^{-3}
	h (mg $g^{-1}min^{-1}$)	5.39	7.77	8.88	9.97
	$q_{e\ exp}$ (mg g^{-1})	41.11	45.30	47.90	49.89
	$q_{e\ theo}$ (mg g^{-1})	43.64	48.31	50.76	52.63
	R^2	0.9979	0.9985	0.9989	0.9990
	SSE (%)	0.84	1.00	0.97	0.91

3.5 Adsorption Mechanism

Adsorption is a physicochemical process whose mechanism is normally characterized by four steps; (i) migration of solute from bulk of the solution to the adsorbent surface (bulk diffusion); (ii) external mass transfer of solute across the liquid film to the adsorbent exterior surface (film diffusion); (iii) solute transport from exterior surface into the pores of the adsorbent (intraparticle diffusion or pore diffusion) and; (iv) adsorption of solute on active sites in inner and outer surfaces of adsorbent [54]. The first step is generally presumed to be rapid and therefore cannot be considered as rate-controlling step. For this reason, film diffusion and pore diffusion are regarded as prominent rate determining factors. The pseudo first order and pseudo second order models are limited in explaining the roles of diffusion (film diffusion; pore diffusion or both) in the sorption process. In order to elucidate the dominating mechanism of Cr(VI) adsorption onto ACBA, particularly, the potential rate limiting step, the experimental data were analyzed using intraparticle diffusion and Boyd models.

3.7.1. Intraparicle diffusion model

Intraparticle diffusion model is an important kinetic model commonly used to study the diffusion mechanism of adsorption. The intraparticle diffusion equation [55] is given by:

$$q_t = k_{id}t^{\frac{1}{2}} + C \qquad (17)$$

where k_{id} (mg g^{-1} $min^{-1/2}$) is the intraparticle diffusion rate constant, and qt (mg g^{-1}) is the amount of metal adsorbed at time t (min). The value of C gives an insight about the boundary layer thickness, the smaller the intercept the lower the boundary layer effect [56]. The values of k_{id}, C and R^2 are summarized in Table 2.

Table 2. Intraparticle diffusion model parameters for Cr(VI) adsorption

T (K)	K_{id} (gmg^{-1} min^{-1})	C	R^2
303	2.827	16.116	0.7851
313	2.729	21.148	0.7881
323	2.728	23.783	0.7824
333	2.666	26.266	0.7927

Theoretically, intraparticle diffusion can be regarded as rate-controlling step when the plot of qt versus $t^{1/2}$ yield a straight line and zero intercept. From Fig. 10, the resultant plots for different temperatures did not go through the origin and at least three linear segments existed. The multi-linearity implies that that three or more stages occurred in the sorption process. Also, it was indicative of some degree of boundary layer control and this showed that the intraparticle diffusion is not the sole rate-controlling step, both of which could be occurring simultaneously [57]. Meanwhile, the boundary layer effect is augmented with increase in the solution temperature. The first linear segment is the initial rapid adsorption step which is ascribed to the fast diffusion of Cr(VI) from the aqueous phase to the exterior surface of the ACBA. The second segment is a slow adsorption process which could be attributed to the diffusion of the metal into the pores of the adsorbent. In other words, when the external surface became saturated, the adsorbate entered into the pores and were adsorbed by the internal surface.

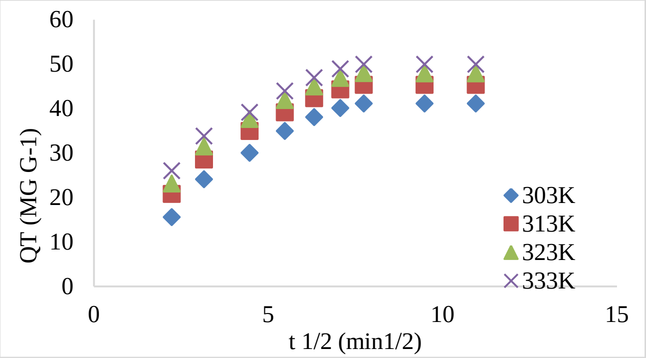

Fig 10. Intraparticle diffusion fit for Cr(VI) uptake by ACBA

The plateau (final segment) is the equilibrium stage where pore diffusion starts to slow down due to extremely low adsorbate concentration in the solution [58].

Table 2. Intraparticle diffusion model parameters for Cr(VI) adsorption

T (K)	K_{id} (gmg^{-1} min^{-1})	C	R^2
303	2.827	16.116	0.7851
313	2.729	21.148	0.7881
323	2.728	23.783	0.7824
333	2.666	26.266	0.7927

3.7.2. Boyd model

It is obvious from Fig. 10 that both intraparticle diffusion and film diffusion influenced the uptake of Cr(VI) by the adsorbent. Boyd model was employed to further examine the kinetic data as to the precise rate controlling step between intraparticle diffusion and film diffusion. The Boyd mathematical model is given by [59]:

$$F = 1 - \frac{6}{\pi^2}\sum_{n=1}^{\infty}\frac{1}{n^2}\exp(-n^2Bt) \qquad (18)$$

$$F = \frac{qt}{qe} \qquad (19)$$

where F represents the fractional attainment of equilibrium at time, t (min), n is the Freundlich constant, Bt is a function of F and qt and qe represent amount of metal adsorbed at time, t, and at equilibrium, repectively.

A simpler relation for computing the value of Bt for each values of F is represented by the following equation [60]:

$$B_t = -0.4977 - \ln(1 - F) \qquad (20)$$

The plot of Bt versus t used to examine the mechanism of adsorption process was depicted in Fig. 11. According to Boyd hypothesis, if the plot exhibits linearity and passes through the origin, then it is a signifier of intraparticle diffusion otherwise film diffusion. From Fig. 11, it can be seen that for all the temperatures studied, Bt versus t plot deviates from the linearity without passing through the origin. This implies that for the studied temperature range, mainly film diffusion dominates the sorption process [61].

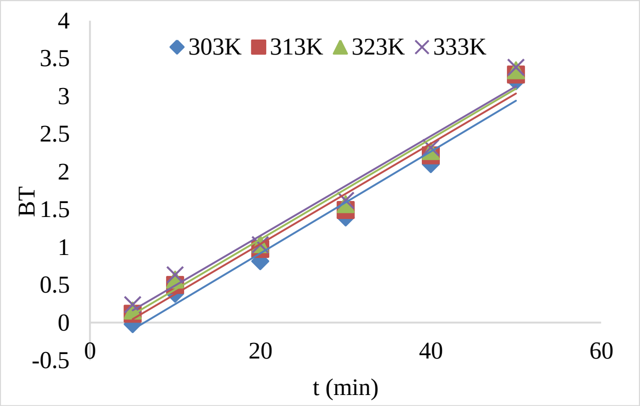

Fig 11. Boyd plot for Cr(VI) adsorption by ACBA

3.8. Thermodynamic and activation parameters

The evaluation of nature of Cr(VI) sorption onto ACBA can be explored by applying Arrhenius equation using the pseudo second order rate constants, k_2 at different temperatures [62].

$$\ln k_2 = \ln A - \left(\frac{E_a}{RT}\right) \quad (21)$$

where E_a is the activation energy (kJ mol^{-1}) of the adsorption; A is the temperature-independent pre-exponential factor, R is the gas constant (0.0008314 kJ mol^{-1}) and T is the temperature (K).

The gradient of the plot of ln k_2 versus 1/T (Fig. 12) can be employed for the estimation of activation energy and the value was given in Table 3. The magnitude of E_a helps in understanding the type of sorption process involved. For physical adsorption, E_a value is normally <40 kJ mol^{-1}, while value >40 kJ mol^{-1} signify chemical adsorption to dominate the process [63]. The value of E_a obtained for the present adsorption system was found to be 7.981 kJ mol^{-1} and therefore physical forces administrate the adsorption of Cr(VI) onto ACBA.

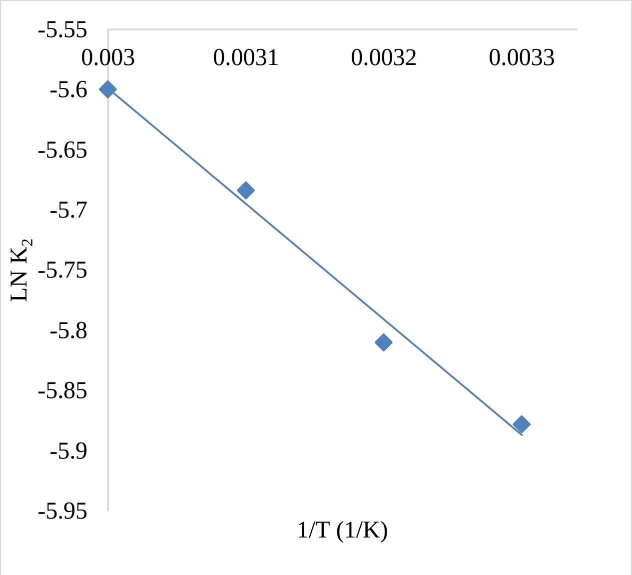

Fig 12. Plot of ln k_2 versus 1/T for the sorption of Cr(VI) onto ACBA

The practicability of the metal adsorption behavior on the adsorbent can be examine through thermodynamic investigation. Thermodynamic quantities such as standard enthalpy change (ΔH°), entropy change (ΔS°) and Gibbs free energy change (ΔG°) can be evaluated using the following equations:

$$K_c = \frac{Co - Ce}{Ce} \quad (22)$$

$$\Delta G = -RT\ln K_c \quad (23)$$

$$\Delta G^o = \Delta H^o - T\Delta S^o \quad (24)$$

$$\ln Kc = -\frac{\Delta Ho}{RT} + \frac{\Delta S^o}{R} \quad (25)$$

where K_c is the standard thermodynamic equilibrium constant, R and T have their usual meanings as mentioned earlier.

Table 3 summarizes the thermodynamic parameters estimated from the plot of ln K_c versus 1/T (Fig. 13). The positive value of enthalpy change is consistent with the endothermic nature of the adsorption process. The negative value of Gibbs free energy change intimates that the Cr(VI) adsorption on ACBA is feasible and spontaneous in nature.

Table 3. Thermodynamic parameters for the adsorption of Cr(VI) onto ACBA

Temp. (K)	E_a(kJ.mol^{-1})	ΔH° (kJ mol^{-1})	ΔS°(kJmol^{-1} K^{-1})	ΔG°(kJ mol^{-1})
303	7.981	64.130	0.224	-3.854
313				-5.894
323				-8.395
333				-10.560

The values of ΔG increase with rising temperatures indicating higher temperature favors Cr(VI) adsorption onto ACBA. The positive value of entropy change reflects a favorable condition for metal adsorption [64].

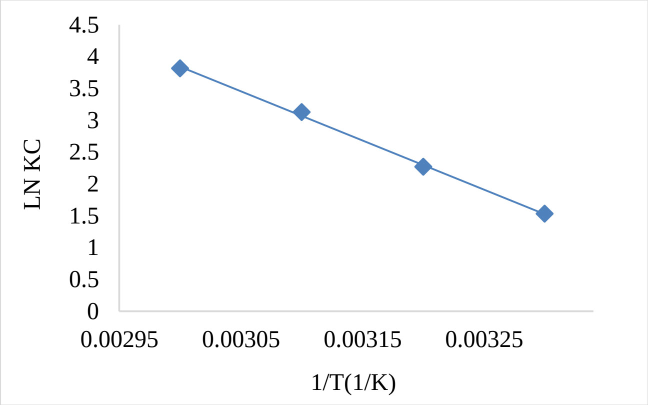

Fig 13. Plot of ln Kc versus 1/T for the adsorption of Cr(VI) onto ACBA

In order to examine the activation parameters (ΔG^*, ΔH^*, ΔG^*) in the transition state of adsorption, ln (k_2/T) was plotted againt 1/T using the Eyring equation [65]:

$$\ln\left(\frac{k_2}{T}\right) = \ln\frac{k_B}{h_p} + \frac{\Delta S^*}{R} - \frac{\Delta H^*}{RT} \quad (26)$$

where k_B stands for Boltzmann constant (1.3807 x 10^{-23} J K^{-1}), h_p is the Planck constant (6.626 x 10^{-34} J s), ΔH^* (kJ mol^{-1}), ΔS^* (kJ mol^{-1}K^{-1}), and ΔG^* (kJ mol^{-1}) are the activation enthalpy, entropy and Gibbs free energy, respectively.

From Fig. 14, the values of ΔH^* and ΔS^* were estimated from the slope and intercept, and then ΔG^* was calculated accordingly (Table 4).

Table 4. Activation parameters for the adsorption of Cr(VI) onto ACBA

Temperature (K)	ΔH^* (kJ mol^{-1})	ΔS^* (kJmol^{-1} K^{-1})	ΔG^* (kJ mol^{-1})
303	1.621	0.287	-0.085
313			-0.086
323			-0.089
333			-0.091

The positive value of ΔH^* (1.621 kJ mol^{-1}) indicates the endothermic nature of the adsorption. The positive value of ΔS^* (0.287 kJ mol^{-1}K^{-1}) hints that the adsorption proceeds via dissociative mechanism. The negative values of ΔG^* (kJ mol^{-1}) indicate no energy input was required in the adsorption reaction to transform the reactants into activated complex [65].

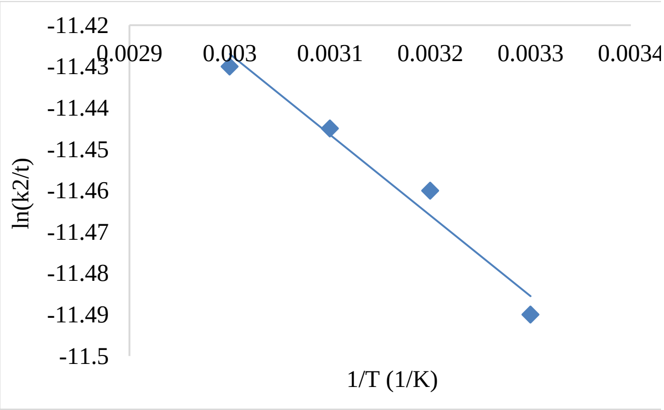

Fig 14. Plot of ln (k_2/T) versus 1/T for the adsorption of Cr(VI) onto ACBA

The isosteric heat of adsorption ($\Delta H_{x,}$ kJ mol^{-1}) is defined as the heat of adsorption obtained at constant quantity of sorbate adsorbed. At constant surface coverage, the isosteric heat of adsorption was estimated using the Clausius-Clapeyron equation [66]:

$$D\frac{(\ln C_e)}{dT} = \frac{\Delta H_x}{RT^2} \tag{27}$$

The value of ΔH_x was determined from the slope of a plot ln C_e versus 1/T (Fig. 15). For physisorption, ΔH_x should be less than 80 kJ mol^{-1} and for chemisorption it ranges between 80 and 400 kJ mol^{-1} [67]. In this study, the value of ΔH_x was 66.345 kJ mol^{-1}, indicating that the Cr(VI) adsorption process is controlled by weak physical forces.

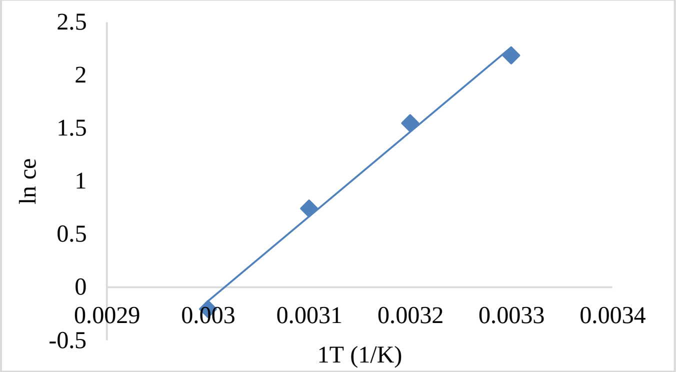

Fig. 15. Plot of ln Ce against 1/T for the adsorption of Cr(VI) onto ACBA

3.9. Regeneration Studies

For industrial application of the adsorption process, the two key factors that need to be taken into account are the low cost and reusability of the adsorbent material. The reusability not only significantly lower the overall cost of the process but also lessen the hazard that might be created by disposal of the spent adsorbent bearing the target contaminant [68,69]. A number of regeneration techniques including chemical, steam, ozone, oxidative, vacuum, microwave and bioregeneration have been applied to recover and recycle spent adsorbents [70]. In this study, we opted for chemical regeneration because of its comparatively low cost and zero adsorbent loss.

3.9.1. Desorption process

Fig. 16 demonstrates that desorption efficiency of Cr(VI) by NaOH (65.08%) was dramatically higher than any other regeneration solution. This type of trend was anticipated due to the fact that Cr(VI) predominantly exist in the form of $HCrO_4^-$ at pH 2.0 [71]. Therefore, in basic medium, the concentration of hydroxide ions (OH^-) was sufficient to compete with the Cr(VI) anions for adsorption sites making the desorption process feasible. This finding indicates that Cr(VI) was adsorbed by heterogeneous sorption site mechanism, which likely involved electrostatic interaction, H-bonding and hydrophobic interaction [72].

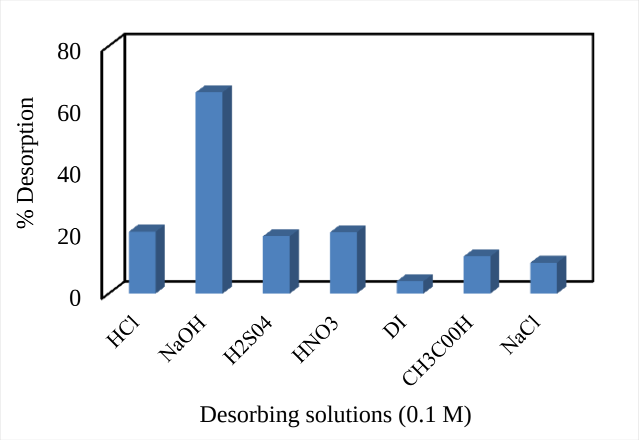

Fig 16. Desorption characteristics of Cr(VI) under different desorbing solutions (conditions: concentration = 0.1 M, adsorbent mass = 0.1 g; agitation speed = 150 rpm, contact time = 30 min)

3.9.2. *Effect of contact time and solution concentration*

Fig. 17 represented the variation of desorption efficiency with contact time at different concentration of desorbing solution. The result indicates that the amount of Cr(VI) recovered increases with an increase in contact time before equilibrium was attained after just 15 min. Of interest, it was reported that most of the sorbates adsorbed on surfaces, desorbed within short period of time if there was no internal diffusion resistance to the metal inside the adsorbent [73]. This may be further proof that the adsorption of the chromium by the ACBA is not largely influenced by intraparticle diffusion, which is in compliance with the Boyd and intraparticle diffusion models mentioned. It is also observed that percentage recovery of Cr(VI) increased with increase in concentration of desorbing solution. This is because, at high concentration of desorbing solution (NaOH), the abundance of hydroxyl ions (OH^{-1}) enhances hindrance to diffusion of Cr(VI) anions, thereby improving detachment of the anion from the ACBA surface [74].

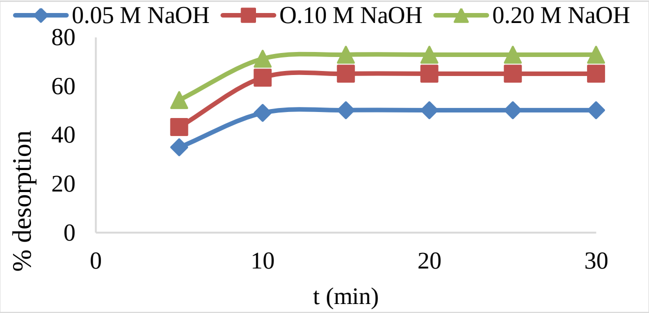

Fig. 17. Effect of contact time and concentration on Cr(VI) recovery (conditions: adsorbent mass = 0.1 g; agitation speed = 150 rpm, solution volume = 100 mL)

3.7.3. *Reusability studies*

Reusability of ACBA was illustrated in Fig. 18. At the first adsorption equilibrium, the maximum removal efficiency was 94%. It was observed that with the increase in cycle number, the adsorption/desorption efficiency showed a trend of decreasing. The efficiency was found to be appreciably high up to the six cycles reflecting the high stability and economic viability of the adsorbent. This finding affirms that the ACBA can be useful for application in a continuous industrial scale operation.

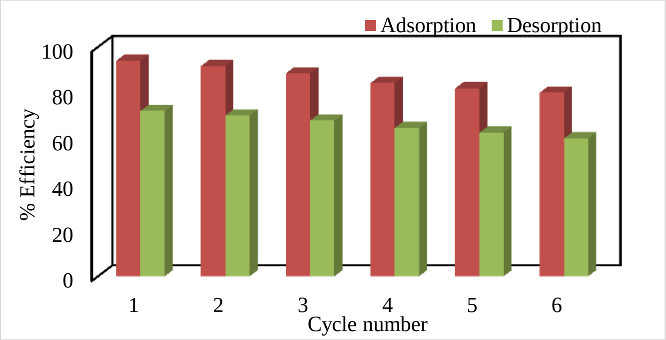

Fig 18. Reusability of ACBA for consecutive adsorption-desorption cycles of Cr(VI) (conditions: adsorbent mass = 0.1 g; agitation speed = 150 rpm, solution volume = 100 mL)

4. Conclusion

A biomass-based activated carbon has been prepared from *Balanites aegyptiaca* seed shell via chemical activation technique, characterized and applied for the removal of hexavalent chromium from simulated wastewater. The characterization of the adsorbent has been achieved via FTIR, SEM-EDS, BET and XRD techniques. Experimental data showed that the adsorption capacity was dependent on operating variables such as pH, adsorbent amount, contact time and temperature. Kinetic studies indicated that the pseudo second order model was able to provide a realistic description of the adsorption kinetics. It was also observed that film diffusion played dominant role in the adsorption process. The adsorption activation energy evaluated using kinetic data suggested physical nature of Cr(VI) adsorption onto ACBA. Thermodynamic analysis confirmed that the adsorption of Cr(VI) onto ACBA was spontaneous and endothermic in nature. The NaOH offers the highest recovery among the employed desorbing solutions and the regenerated adsorbent could be reused for at least six times maintaining an adsorption efficiency of 80.10%. Altogether, the ACBA showed high adsorptive performance and proper kinetics, indicating the suitability of its application in wastewater treatment.

Conflict of Interest

The authors declare that they have no conflict of interest

References

1. Sharma YC. Adsorption characteristics of a low-cost activated carbon for the reclamation of colored effluents containing malachite green. *Journal of Chemical & Engineering Data*. 2011;56(3):478-484.
2. Hassan R, Arida H, Montasser M, Abdel Latif N. Synthesis of new Schiff base from natural products for remediation of water pollution with heavy metals in industrial areas. *Journal of Chemistry*. 2013, Article ID: 240568.
3. ŞENOL ZM, ŞİMŞEK S. Removal of Pb2+ ions from aqueous medium by using chitosan-diatomite composite: equilibrium, kinetic and thermodynamic studies. *Journal of the Turkish Chemical Society Section A: Chemistry*. 2020;7(1):307-318.
4. IPCS (International Programme on Chemical Safety). Chromium, Environmental Health Criteria, WHO, Geneva. 1998: 61.
5. Pradhan D, Sukla LB, Sawyer M, Rahman PK. Recent bioreduction of hexavalent chromium in wastewater treatment: a review. *Journal of Industrial and Engineering Chemistry*. 2017;55:1-20.
6. Katz SA. The analytical biochemistry of chromium. *Environmental health perspectives*. 1991;92:13-6.
7. Miretzky P, Cirelli AF. Cr (VI) and Cr (III) removal from aqueous solution by raw and modified lignocellulosic materials: a review. *Journal of hazardous materials*. 2010;180(1-3):1-9.
8. Zhao Y, Yang S, Ding D, Chen J, Yang Y, Lei Z, Feng C, Zhang Z. Effective adsorption of Cr (VI) from aqueous solution using natural Akadama clay. *Journal of colloid and interface science*. 2013;395:198-204.
9. Al-Othman ZA, Ali R, Naushad M. Hexavalent chromium removal from aqueous medium by activated carbon prepared from peanut shell: adsorption kinetics, equilibrium and thermodynamic studies. *Chemical Engineering Journal*. 2012;184:238-247.
10. Babel S, Kurniawan TA. Cr (VI) removal from synthetic wastewater using coconut shell charcoal and commercial activated carbon modified with oxidizing agents and/or chitosan. *Chemosphere*. 2004;54(7):951-967.
11. IARC (International Agency for Research on Cancer), IARC monographs on the evaluation of carcinogenic risks to human: overall evaluation of carcinogenicity. An updating of IARC monographs, vols. 1-2, supplement 7, WHO, Lyon, France, 1987.
12. Yang J, Yu M, Chen W. Adsorption of hexavalent chromium from aqueous solution by activated carbon prepared from longan seed: Kinetics, equilibrium and thermodynamics. *Journal of industrial and engineering chemistry*. 2015;21:414-422.
13. Zhao Z, An H, Lin J, Feng M, Murugadoss V, Ding T, Liu H, Shao Q, Mai X, Wang N, Gu H. Progress on the photocatalytic reduction removal of chromium contamination. *The Chemical Record*. 2019;19(5):873-82.
14. Gupta S, Babu BV. Removal of toxic metal Cr (VI) from aqueous solutions using sawdust as adsorbent: Equilibrium, kinetics and regeneration studies. *Chemical Engineering Journal*. 2009;150(2-3):352-365.
15. Parlayici Ş, Pehlivan E. Comparative study of Cr (VI) removal by bio-waste adsorbents: equilibrium, kinetics, and thermodynamic. *Journal of Analytical Science and Technology*. 2019;10(1):1-8.
16. Bayuo J, Pelig-Ba KB, Abukari MA. Adsorptive removal of chromium (VI) from aqueous solution unto groundnut shell. *Applied Water Science*. 2019;9(4):1-11.
17. Bhatnagar A, Kumar E, Sillanpää M. Fluoride removal from water by adsorption—a review. *Chemical engineering journal*. 2011;171(3):811-840.
18. Hegazi HA. Removal of heavy metals from wastewater using agricultural and industrial wastes as adsorbents. *HBRC journal*. 2013;9(3):276-82.
19. Loganathan P, Vigneswaran S, Kandasamy J, Naidu R. Defluoridation of drinking water using adsorption processes. *Journal of hazardous materials*. 2013;248:1-9.
20. Sharma PK, Ayub S, Tripathi CN. Isotherms describing physical adsorption of Cr (VI) from aqueous solution using various agricultural wastes as adsorbents. *Cogent Engineering*. 2016;3(1):1186857.
21. Velazquez-Jimenez LH, Hurt RH, Matos J, Rangel-Mendez JR. Zirconium–carbon hybrid sorbent for removal of fluoride from water: oxalic acid mediated Zr (IV) assembly and adsorption mechanism. *Environmental science & technology*. 2014;48(2):1166-1174.
22. Bello OS, Adegoke KA, Olaniyan AA, Abdulazeez H. Dye adsorption using biomass wastes and natural adsorbents: overview and future prospects. *Desalination and Water Treatment*. 2015;53(5):1292-1315.
23. El-Hendawy ANA, Samara SE, Giris BS. Adsorption characteristics of activated carbons obtained from corncorbs. *Colloids and Surfaces A: Physicochemical and Engineering Aspects.* 2001:180:209-221.
24. Nasri NS, Hamza UD, Ismail SN, Ahmed MM, Mohsin R. Assessment of porous carbons derived from sustainable palm solid waste for carbon dioxide capture. *Journal of Cleaner Production*. 2014;71:148-157.
25. Rai MK, Giri BS, Nath Y, Bajaj H, Soni S, Singh RP, Singh RS, Rai BN. Adsorption of hexavalent chromium from aqueous solution by activated carbon prepared from almond shell: kinetics, equilibrium and thermodynamics study. Journal of Water Supply: *Research and Technology-Aqua*. 2018;67(8):724-737.
26. Labied R, Benturki O, Eddine Hamitouche AY, Donnot A. Adsorption of hexavalent chromium by activated carbon obtained from a waste lignocellulosic material (Ziziphus jujuba cores): Kinetic, equilibrium, and thermodynamic study. *Adsorption Science & Technology*. 2018;36(3-4):1066-99.
27. Kannan A, Thambidurai S. Removal of hexavalent chromium from aqueous solution using activated carbon derived from palmyra palm fruit seed. *Bulletin of the Chemical Society of Ethiopia*. 2008;22(2):183-196.
28. Mullick A, Moulik S, Bhattacharjee S. Removal of hexavalent chromium from aqueous solutions by low-cost rice husk-based activated carbon: kinetic and thermodynamic studies. *Indian Chemical Engineer*. 2018;60(1):58-71.
29. Azaman SH, Afandi A, Hameed BH, Din AM. Removal of malachite green from aqueous phase using coconut shell activated carbon: Adsorption, desorption, and reusability studies. *Journal of Applied Science and Engineering*. 2018;21(3):317-330.
30. Razavi Mehr M, Fekri MH, Omidali F, Eftekhari N, Akbari-adergani B. Removal of chromium (VI) from wastewater by palm kernel shell-based on a green method. *Journal of Chemical Health Risks*. 2019;9(1):75-86.

31. Nethaji S, Sivasamy A. Removal of hexavalent chromium from aqueous solution using activated carbon prepared from walnut shell biomass through alkali impregnation processes. *Clean Technologies and Environmental Policy*. 2014;16(2):361-368.
32. Enniya I, Rghioui L, Jourani A. Adsorption of hexavalent chromium in aqueous solution on activated carbon prepared from apple peels. *Sustainable Chemistry and Pharmacy*. 2018;7:9-16.
33. Dula T, Siraj K, Kitte SA. Adsorption of hexavalent chromium from aqueous solution using chemically activated carbon prepared from locally available waste of bamboo (*Oxytenanthera abyssinica*). *International Scholarly Research Notices*. 2014;2014.
34. Pakade VE, Nchoe OB, Hlungwane L, Tavengwa NT. Sequestration of hexavalent chromium from aqueous solutions by activated carbon derived from Macadamia nutshells. *Water Science and Technology*. 2017;75(1):196-206.
35. Yunusa U, Ibrahim MB. Reclamation of malachite green-bearing wastewater using desert date seed shell: adsorption isotherms, desorption and reusability studies. *Chemsearch Journal*. 2019;10(2):112-22.
36. Yunusa U, Bishir U, Ibrahim MB. Kinetic and thermodynamic studies of malachite green adsorption using activated carbon prepared from desert date seed shell. *Algerian Journal of Engineering and Technology*. 2020;2:37-45.
37. Wang X, Wang S, Yin X, Chen J, Zhu L. Activated carbon preparation from cassava residue using a two-step KOH activation: preparation, micropore structure and adsorption capacity. *Journal of Biobased Materials and Bioenergy.* 2014;8(1):35-42.
38. Hameed BH, Din AM, Ahmad AL. Adsorption of methylene blue onto bamboo-based activated carbon: kinetics and equilibrium studies. *Journal of hazardous materials*. 2007;141(3):819-825.
39. Liu J, Li WY, Liu Y, Zeng Q, Hong S. Titanium (IV) hydrate based on chitosan template for defluoridation from aqueous solution. *Applied surface science*. 2014;293:46-54.
40. Debnath S, Ghosh UC. Nanostructured hydrous titanium (IV) oxide: synthesis, characterization and Ni (II) adsorption behavior. *Chemical engineering journal*. 2009;152(2-3):480-491.
41. Khan MM, Rahman MW, Ong HR, Ismail AB, Cheng CK. Tea dust as a potential low-cost adsorbent for the removal of crystal violet from aqueous solution. *Desalination and Water Treatment*. 2016;57(31):14728-38.
42. Ali I, Peng C, Ye T, Naz I. Sorption of cationic malachite green dye on phytogenic magnetic nanoparticles functionalized by 3-marcaptopropanic acid. *RSC advances*. 2018;8(16):8878-8897.
43. Baral SS, Das SN, Rath P. Hexavalent chromium removal from aqueous solution by adsorption on treated sawdust. *Biochemical Engineering Journal*. 2006;31(3):216-222.
44. Inam EI, Etim UJ, Akpabio EG, Umoren SA. Simultaneous adsorption of lead (II) and 3, 7-Bis (dimethylamino)-phenothiazin-5-ium chloride from aqueous solution by activated carbon prepared from plantain peels. *Desalination and Water Treatment*. 2016;57(14):6540-6553.
45. Akar T, Tunali S. Biosorption performance of Botrytis cinerea fungal by-products for removal of Cd (II) and Cu (II) ions from aqueous solutions. *Minerals Engineering*. 2005;18(11):1099-1109.
46. Crini G, Peindy HN, Gimbert F, Robert C. Removal of CI Basic Green 4 (Malachite Green) from aqueous solutions by adsorption using cyclodextrin-based adsorbent: kinetic and equilibrium studies. *Separation and Purification Technology*. 2007;53(1):97-110.
47. Mohan D, Singh KP, Singh VK. Trivalent chromium removal from wastewater using low cost activated carbon derived from agricultural waste material and activated carbon fabric cloth. *Journal of hazardous materials*. 2006;135(1-3):280-295.
48. Hu Z, Lei L, Li Y, Ni Y. Chromium adsorption on high-performance activated carbons from aqueous solution. *Separation and Purification Technology*. 2003;31(1):13-18.
49. Azizian S. Kinetic models of sorption: a theoretical analysis. *Journal of colloid and Interface Science*. 2004;276(1):47-52.
50. Aksakal O, Ucun H. Equilibrium, kinetic and thermodynamic studies of the biosorption of textile dye (Reactive Red 195) onto Pinus sylvestris L. *Journal of hazardous materials*. 2010;181(1-3):666-672.
51. McKay G, Ho YS, Ng JC. Biosorption of copper from waste waters: a review. *Separation and Purification Methods*. 1999;28(1):87-125.
52. Ho YS, McKay G. Kinetic models for the sorption of dye from aqueous solution by wood. *Process Safety and Environmental Protection*. 1998;76(2):183-191.
53. Tewari N, Vasudevan P, Guha BK. Study on biosorption of Cr (VI) by Mucor hiemalis. *Biochemical Engineering Journal*. 2005;23(2):185-192.
54. Ma J, Yu F, Zhou L, Jin L, Yang M, Luan J, Tang Y, Fan H, Yuan Z, Chen J. Enhanced adsorptive removal of methyl orange and methylene blue from aqueous solution by alkali-activated multiwalled carbon nanotubes. *ACS applied materials & interfaces*. 2012;4(11):5749-5760.
55. Weber WJ, Morris JC. Kinetics of adsorption on carbon from solution. *Journal of the sanitary engineering division*. 1963;89(2):31-60.
56. Bello OS, Ahmad MA. Coconut (Cocos nucifera) shell based activated carbon for the removal of malachite green dye from aqueous solutions. *Separation Science and Technology*. 2012;47(6):903-912.
57. Arami M, Limaee NY, Mahmoodi NM. Evaluation of the adsorption kinetics and equilibrium for the potential removal of acid dyes using a biosorbent. *Chemical Engineering Journal*. 2008;139(1):2-10.
58. Gorzin F, Bahri Rasht Abadi MM. Adsorption of Cr (VI) from aqueous solution by adsorbent prepared from paper mill sludge: Kinetics and thermodynamics studies. *Adsorption Science & Technology*. 2018;36(1-2):149-69.
59. Boyd GE, Adamson AW, Myers JLS. The exchange of Ions from Aqueous Solution by Organic Zeolites, II: Kinetic. *Journal of the American Chemical Society*, 1947;69:2836-2848.
60. Reichenberg D. Properties of ion-exchange resins in relation to their structure. III. Kinetics of exchange. *Journal of the American Chemical Society*. 1953;75(3):589-97.

61. Banerjee S, Sharma GC, Gautam RK, Chattopadhyaya MC, Upadhyay SN, Sharma YC. Removal of Malachite Green, a hazardous dye from aqueous solutions using Avena sativa (oat) hull as a potential adsorbent. *Journal of Molecular Liquids*. 2016;213:162-172.
62. Parashar K, Ballav N, Debnath S, Pillay K, Maity A. Hydrous TiO 2@ polypyrrole hybrid nanocomposite as an efficient selective scavenger for the defluoridation of drinking water. *RSC advances*. 2016;6(101):99482-99495.
63. Banerjee S, Gautam RK, Jaiswal A, Chattopadhyaya MC, Sharma YC. Rapid scavenging of methylene blue dye from a liquid phase by adsorption on alumina nanoparticles. *RSC advances*. 2015;5(19):14425-14440.
64. Liu Y, Liu YJ. Biosorption isotherms, kinetics and thermodynamics. *Separation and purification technology*. 2008;61(3):229-242.
65. Kang HJ, Kim JH. Adsorption kinetics, mechanism, isotherm, and thermodynamic analysis of paclitaxel from extracts of Taxus chinensis cell cultures onto Sylopute. *Biotechnology and bioprocess engineering*. 2019;24(3):513-521.
66. Lim YS, Kim JH. Isotherm, kinetic and thermodynamic studies on the adsorption of 13-dehydroxybaccatin III from Taxus chinensis onto Sylopute. *The Journal of Chemical Thermodynamics*. 2017;115:261-268.
67. Saha P, Chowdhury S. Insight into adsorption thermodynamics. *Thermodynamics*. 2011;16:349-64. Available from: http://www.intechopen.com/books/thermodynamics/insight into adsorption thermodynamics.
68. Murphy V, Hughes H, McLoughlin P. Comparative study of chromium biosorption by red, green and brown seaweed biomass. *Chemosphere*. 2008;70(6):1128-1134.
69. Nagashanmugam KB, Srinavasan K. Removal of chromium (VI) from aqueous solutions by chemically modified oil cake carbon. *Indian Journal of Chemical Technology*. 2011;18:207-219.
70. Shahadat M, Isamil S. Regeneration performance of clay-based adsorbents for the removal of industrial dyes: a review. *RSC advances*. 2018;8(43):24571-24587.
71. Alemu A, Lemma B, Gabbiye N, Alula MT, Desta MT. Removal of chromium (VI) from aqueous solution using vesicular basalt: a potential low cost wastewater treatment system. *Heliyon*. 2018;4(7):e00682.
72. Afkhami A, Saber-Tehrani M, Bagheri H. Modified maghemite nanoparticles as an efficient adsorbent for removing some cationic dyes from aqueous solution. *Desalination*. 2010;263(1-3):240-248.
73. Lee SL, Park JH, Kim SH, Kang SW, Cho JS, Jeon JR, Lee YB, Seo DC. Sorption behavior of malachite green onto pristine lignin to evaluate the possibility as a dye adsorbent by lignin. *Applied Biological Chemistry*. 2019;62(1):1-0.
74. Werkneh AA, Habtu NG, Beyene HD. Removal of hexavalent chromium from tannery wastewater using activated carbon primed from sugarcane bagasse: Adsorption/desorption studies. *American Journal of Applied Chemistry*. 2014;2(6):128-35.

Recommended Citation

Yunusa U, Kubo AI, Abdullahi Y, Abdullahi T, Husaini M.,. Hexavalent chromium removal from simulated wastewater using biomass-based activated carbon: kinetics, mechanism, thermodynamics and regeneration studies. *Alg. J. Eng. Tech. 2021, 4:29-44* http://dx.doi.org/10.5281/zenodo.4542410